

## Utilization of Metal Forming Process Mathematical Modelling to Predict the Spring-back of the Dual-phase Steel Stamping

David Koreček (0000-0003-2110-2746), Pavel Solfronk (0000-0002-8310-6825), Jiří Sobotka (0000-0002-6569-6593)

Faculty of Mechanical Engineering, Technical University of Liberec. Studentská 2, 461 17 Liberec. Czech Republic.  
E-mail: david.korecek@tul.cz, pavel.solfronk@tul.cz, jiri.sobotka@tul.cz

Nowadays, the digitalization of the production process is an indispensable part of the stampings production in the pre-series stage, but also as a subsequent support for series production. Automotive producers are under pressure to comply with the ever decreasing CO<sub>2</sub> production standards for cars, which predicates the use of modern material types with an advantageous weight-to-strength ratio. This paper focuses on the use of mathematical modelling in a numerical simulation environment to predict the deformation process and subsequent material spring-back of dual-phase steel DP500. The material data and characteristics are used to define the material computational model in numerical simulation. The results of the numerical simulations are then compared with the stamping obtained by a real pressing process, where their shape comparison and further evaluation of the used material models and selected parameters are performed.

**Keywords:** Mathematical Modelling, Yield Locus, High Strength Steel, Forming Process, Spring-back

### 1 Introduction

The use of high-strength materials in the automotive industry is predestined primarily for the production of non-visible panels that serve exclusively as deformation zone elements or reinforcing elements of the car body. In view of the requirements about high strength combined with sufficient ductility of the material for the production of shaped stampings, the introduction of new types of materials in the automotive industry is a highly debated topic. Dual-phase steels offer high strength combined with the sufficient ductility for such production. These materials are based on Manganese-silicon alloys with low medium carbon content. From a structural point of view, these materials consist of a ferritic matrix. Inside this matrix, there are small areas of hard martensite (5 to 50% by volume), which may contain retained austenite depending on the chemical composition and processing method or when increased ductility is required at the shear edge. Due to the basic ferritic matrix, the material gives good formability and the hard martensite elements in this matrix provide high strength values. This material is capable of absorbing large amounts of energy. During forming of this material, deformation is concentrated in the lower strength areas of the ferritic phase surrounding the areas of martensite. As a result, this material exhibits relatively high strain hardening during cold forming. The cause of this effect is the stacking of dislocations around the hard martensitic phase areas during the forming process of the material [1–6].

In the case of forming the strength materials, the deformation process is always followed by a relatively significant spring-back of the material. This undesirable effect must be correctly predicted and subsequently eliminated as much as possible, as it fundamentally affects the final shape, dimensional accuracy and stability of the formed part. Numerical support for the production of stampings is nowadays an indispensable standard. However, in order to achieve accurate results of numerical simulations of the forming process and the subsequent spring-back of the material, it is necessary to correctly define the data that enter the numerical simulations in the form of the yield locus, boundary conditions and other parameters of the numerical simulation. In order to determine and subsequently eliminate the spring-back phenomenon itself as accurately as possible, it is necessary to correctly describe the process of material deformation during forming, which is largely influenced by the material computational model, which is defined using selected material characteristics. The following chapters are devoted to the mechanical testing of the material, which is used to obtain the material data used for the definition of the yield locus used in the numerical simulation and, above all, to the numerical simulation of the forming process and the subsequent spring-back of the material. Finally, the results of the numerical simulations are compared and evaluated with respect to the real sheet metal forming process.

## 2 Definition of the yield locus in numerical simulation

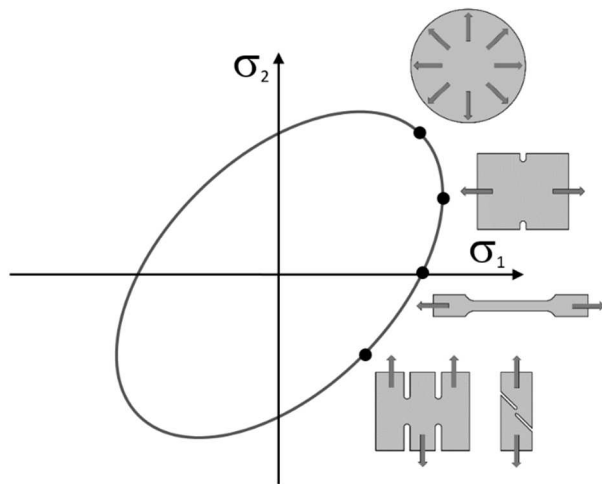


**Fig. 1** Control points of the yield locus in the plane of the main stresses

From the material point of view, it is necessary to define the input material data correctly for an accurate description of the deformation in the numerical simulation environment. The necessary material properties

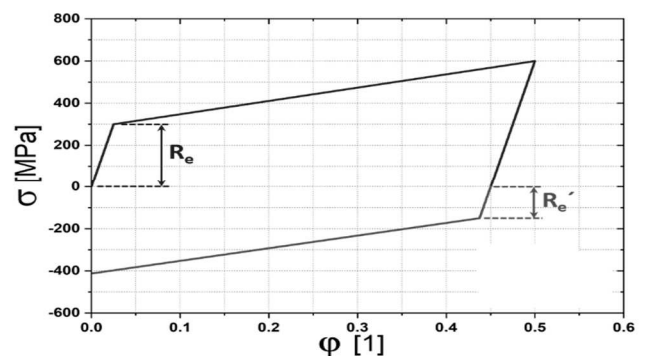
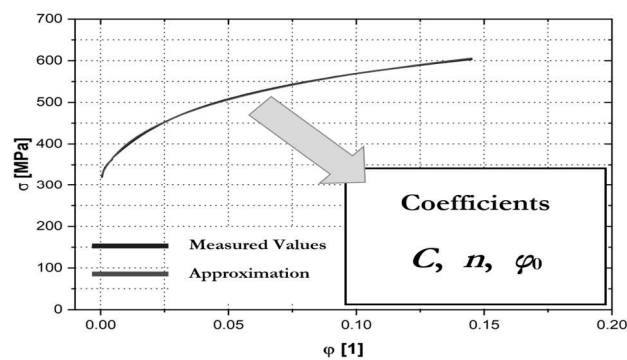


**Fig. 2** Illustration of the stress-strain curve approximation for the definition of the isotropic hardening law (left) and the change in yield strength under fully reversed cyclic loading (right)

The kinematic hardening law used during the deformation (so-called "Yoshida" law), takes into account the change in yield stress of the material under fully reversed loading – tensile and compression (see Fig. 2 – right). This effect is generally called as the "Bauschinger effect" and as a consequence it causes a change in the position of the yield locus boundary during plastic deformation of the material. The definition of this model is performed by means of the "fitted" constants obtained by approximating the stress-strain curve from a cyclic test under uniaxial fully reversed cyclic loading. The advantage of the kinematic "Yoshida" hardening law is precisely taking into account the displacement of the yield locus boundary position during the the deformation computation in the numerical simulation of the material forming process [7].

## 3 Experimental part

and characteristics are obtained through selected material testing. The observed stress-strain behaviour of the material is used to define the yield locus of the material model, where the boundary of the yield locus is defined by control points that represent the stress values obtained from the selected tests. (see Fig. 1) [7, 8].

During deformation, the material undergoes strain hardening, which can be described by an isotropic or kinematic hardening law. The isotropic hardening of the material is described by a stress-strain curve obtained from a static tensile test in the reference direction  $0^\circ$  with respect to the rolling direction (see Fig. 2 – left). Approximation coefficients obtained through the Krupkowski law are used to define this hardening law, see equation (1) [7, 8].

$$\sigma = C \cdot (\varphi_{pl} + \varphi_0)^n \quad (1)$$

Where:

$\sigma$ ... True stress [MPa],

$C$ ... Strength coefficient [MPa],

$n$ ... Strain hardening exponent [1],

$\varphi_{pl}$ ... Plastic true strain [1],

$\varphi_0$ ... Offset of true strain [1].

This chapter deals with the implementation of relevant mechanical testing results into the numerical simulation environment in the software PAM-STAMP 2G. The material data and characteristics enter the simulation process in the form of a material card, where a computational model is selected, an yield locus is defined and finally a material hardening model used during deformation is defined. The selected yield locus are compared with each other. Moreover, there are also compared results from the simulation results with the real stamping process.

To define the relevant yield locus in the numerical simulation, mechanical material testing was carried out – see Fig. 1. In Fig. 3 are summarized the final stress-strain curves measured by the static tensile test with subsequent approximation acc. to Krupkowski law.

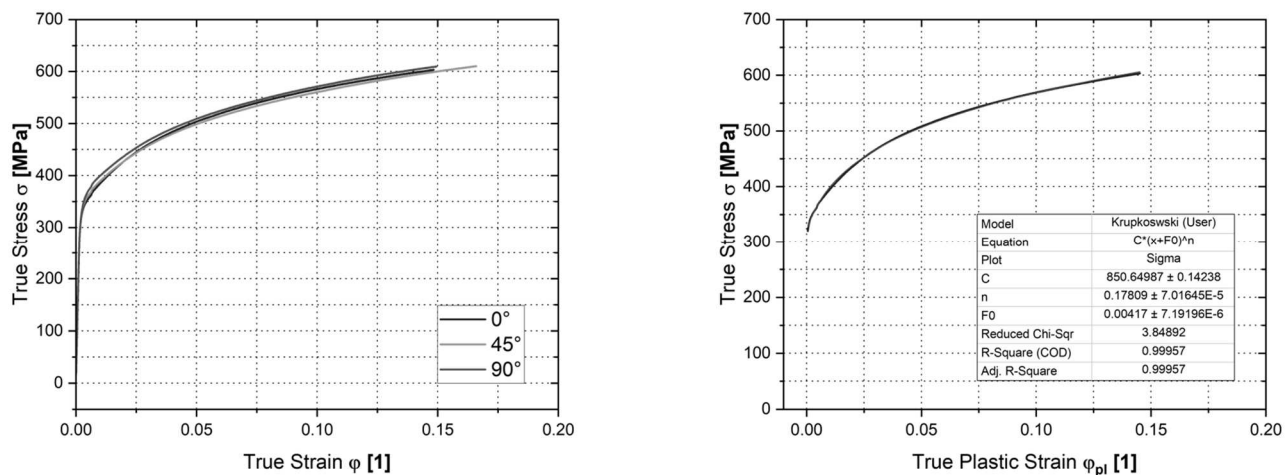


**Fig. 3** Stress-strain curves from the static tensile test for directions  $0^\circ$ ,  $45^\circ$  and  $90^\circ$  regarding the rolling direction (left) and approximation of the stress-strain curve in the reference direction  $0^\circ$  (right)

In Fig. 4 are shown the final dependences true stress vs true strain for the equi-biaxial loading of material as well as Krupkowski approximation of such

stress-strain curve.

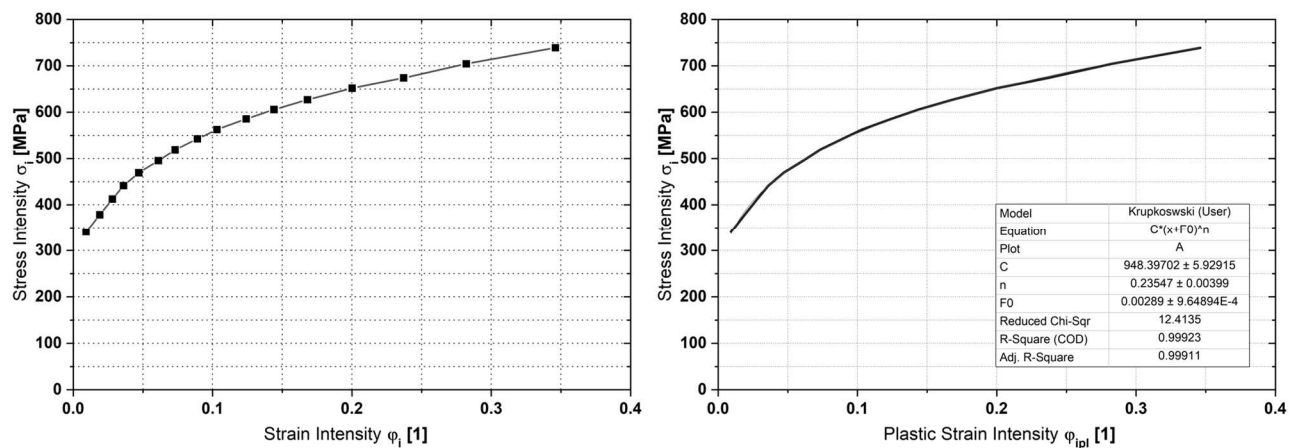


**Fig. 4** Stress-strain curve from the equi-biaxial test (left) and approximation of such curve (right)

In Fig. 5 are shown the final dependences true stress vs true strain measured from the plane strain test.

There is also shown the Krupkowski approximation in the reference direction  $0^\circ$ .

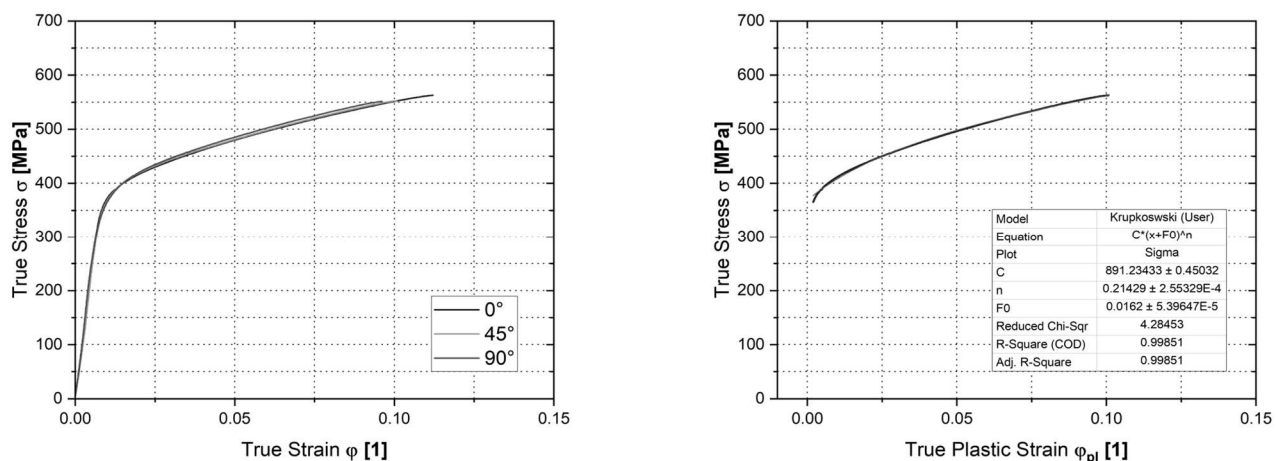
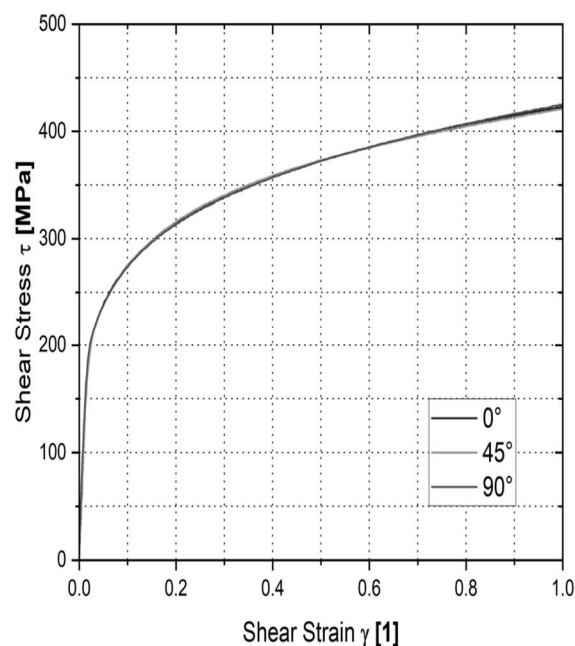


**Fig. 5** Stress-strain curves from the plane strain test for directions  $0^\circ$ ,  $45^\circ$  and  $90^\circ$  regarding the rolling direction (left) and approximation of the stress-strain curve in the reference direction  $0^\circ$  (right)

Fig. 6 illustrates the final dependences shear stress vs shear strain measured from the shear test. Again.



Krupkowski approximation of such stress-strain curve in the reference direction 0° is shown there as well.

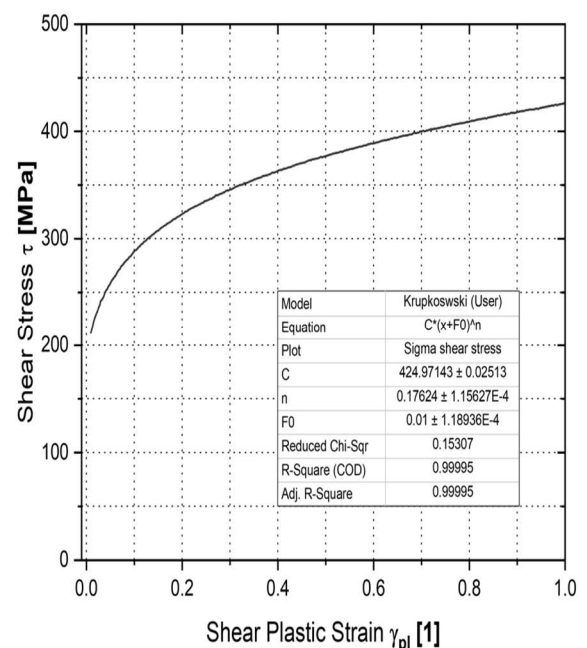


**Fig. 6** Stress-strain curves from the shear test for directions 0°, 45° and 90° regarding the rolling direction (left) and approximation of the stress-strain curve in the reference direction 0° (right)

The measured data and stress characteristics of the material are used to define the material card in the software PAM-STAMP 2G. First, the material type must be selected as well as basic material characteristics – e.g. Young's modulus  $E$ , density  $\rho$  and Poisson's ratio  $\nu$  - see Fig. 7.

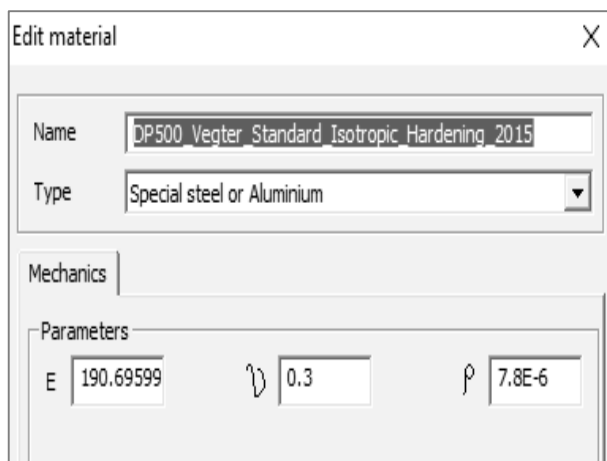


**Fig. 7** Defininition of the basic material characteristics in the sw PAM-STAMP 2G

Next, the material model that controls the choice of the yield locus must be selected - see Fig. 8. Determined stress characteristics of the material are always given here as a ratio to the reference value of the hardenign curve from the static tensile test in the direction 0° - relative to the rolling direction.

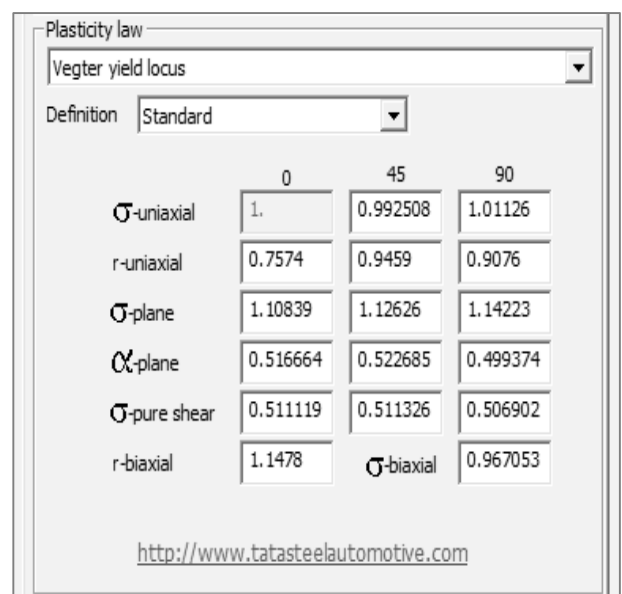


**Fig. 8** Choice of yield locus (plasticity law) and definon of the relevant yield locus in the material card - sw PAM-STAMP 2G

As described above, it is also necessary to define a material hardening law during its deformation. First, there was used the definition of isotropic hardening. This model is defined using the coefficients  $C$ ,  $n$  and  $\varphi_0$ , determined from approximation of the stress-strain from static tensile test in the reference direction 0° with respect to the rolling direction - see Fig. 9.

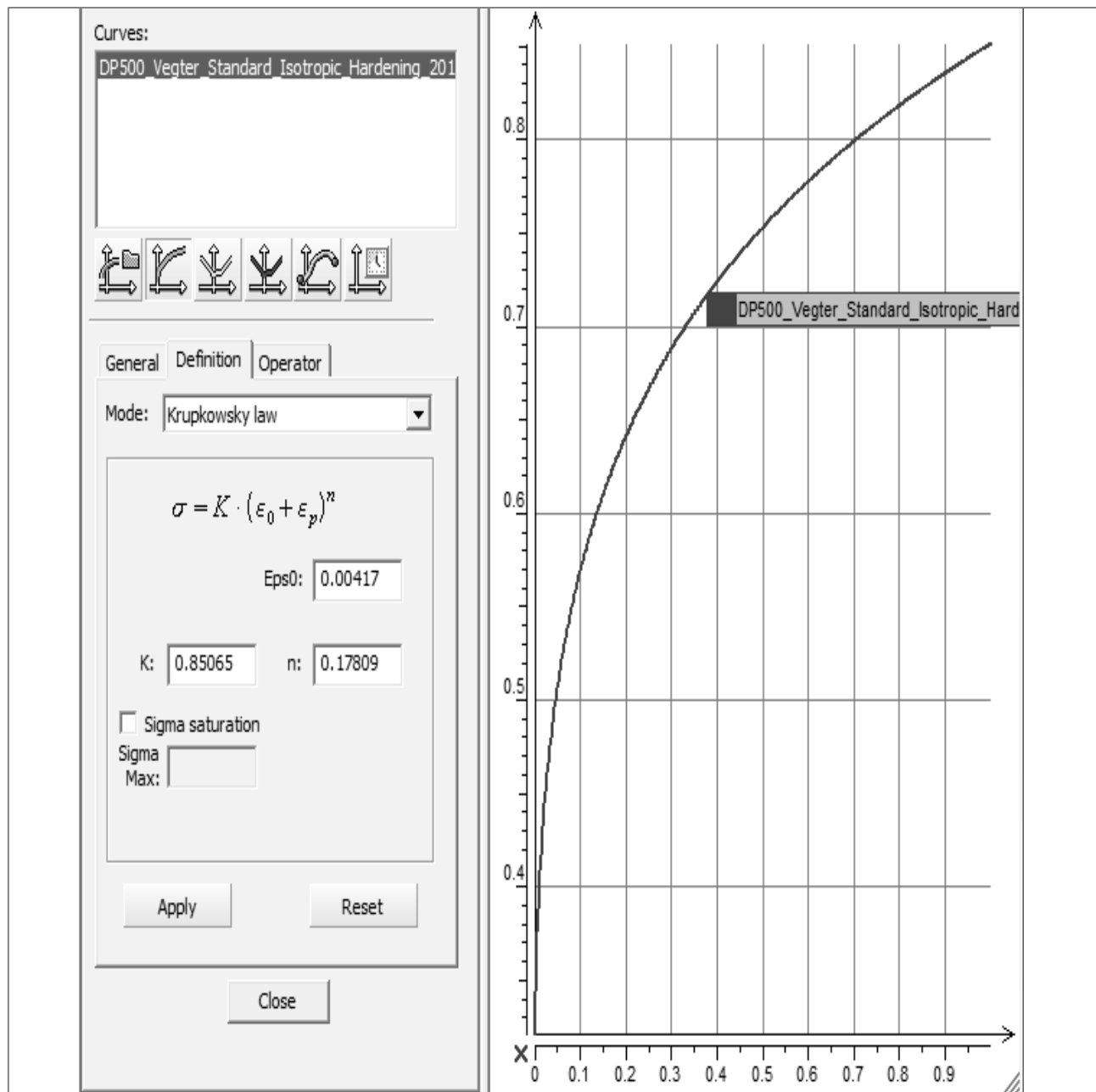


**Fig. 9** Definition of the isotropic hardening law – sw PAM-STAMP 2G

In the case of definition the kinematic hardening law, the influence of so-called Bauschinger effect must be defined and described. Here, it is necessary to perform a cyclic test with uniaxial loading under the reversed tension and compression. As a result from this test, there is stress-strain curve in the form of hysteresis loops – see Fig. 10.

This curve needs to be further approximated to obtain selected constants that are used to define the kinematic "Yoshida" hardening law in the sw PAM-STAMP 2G. This approximation is carried out in collaboration with company MECAS ESI GROUP using the licensed sw MatPara – see Fig. 11.

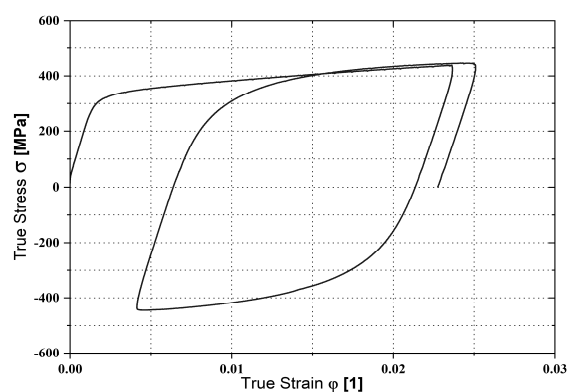


**Fig. 10** Stress-strain curve from the cyclic test

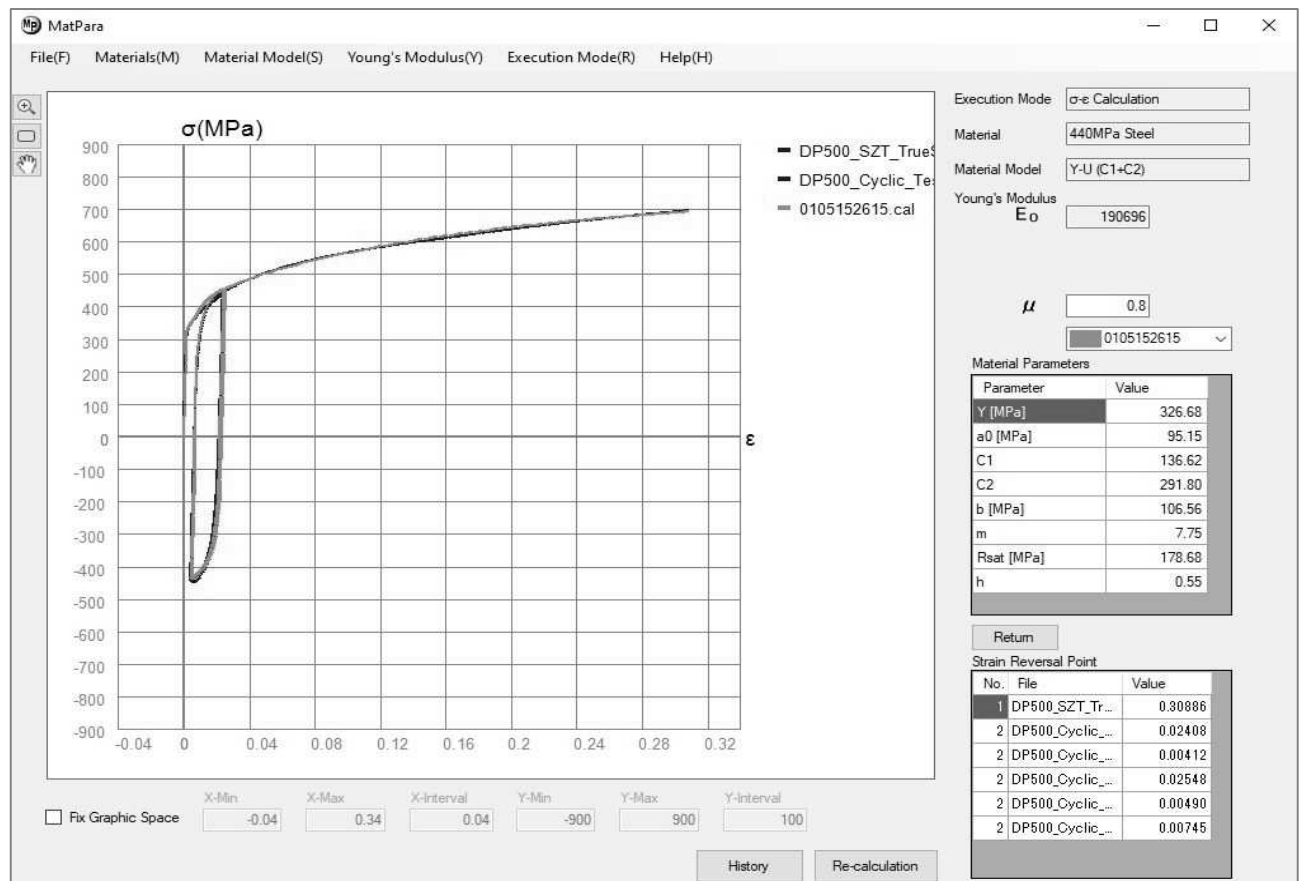


Fig. 11 Illustration of fitting constants for „Yoshida“ hardenign law – sw MatPara

Determiend “fitted” constants are subsequently used to define the kinematic hardening law in the re-

leant material card of sw PAM-STAMP 2G. Definition of the kinematic hardening law is shown in Fig. 12.

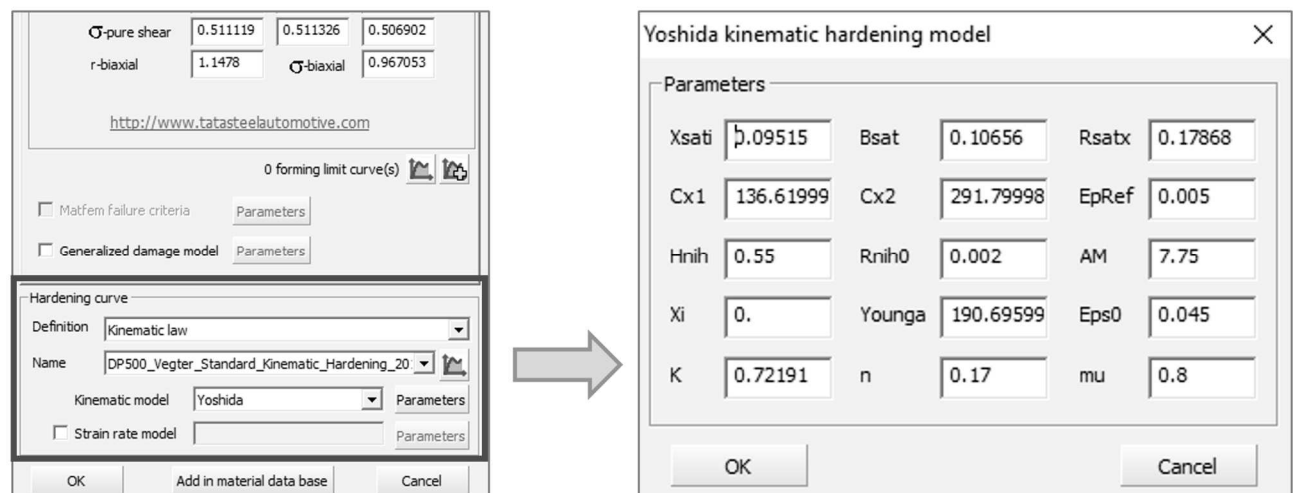
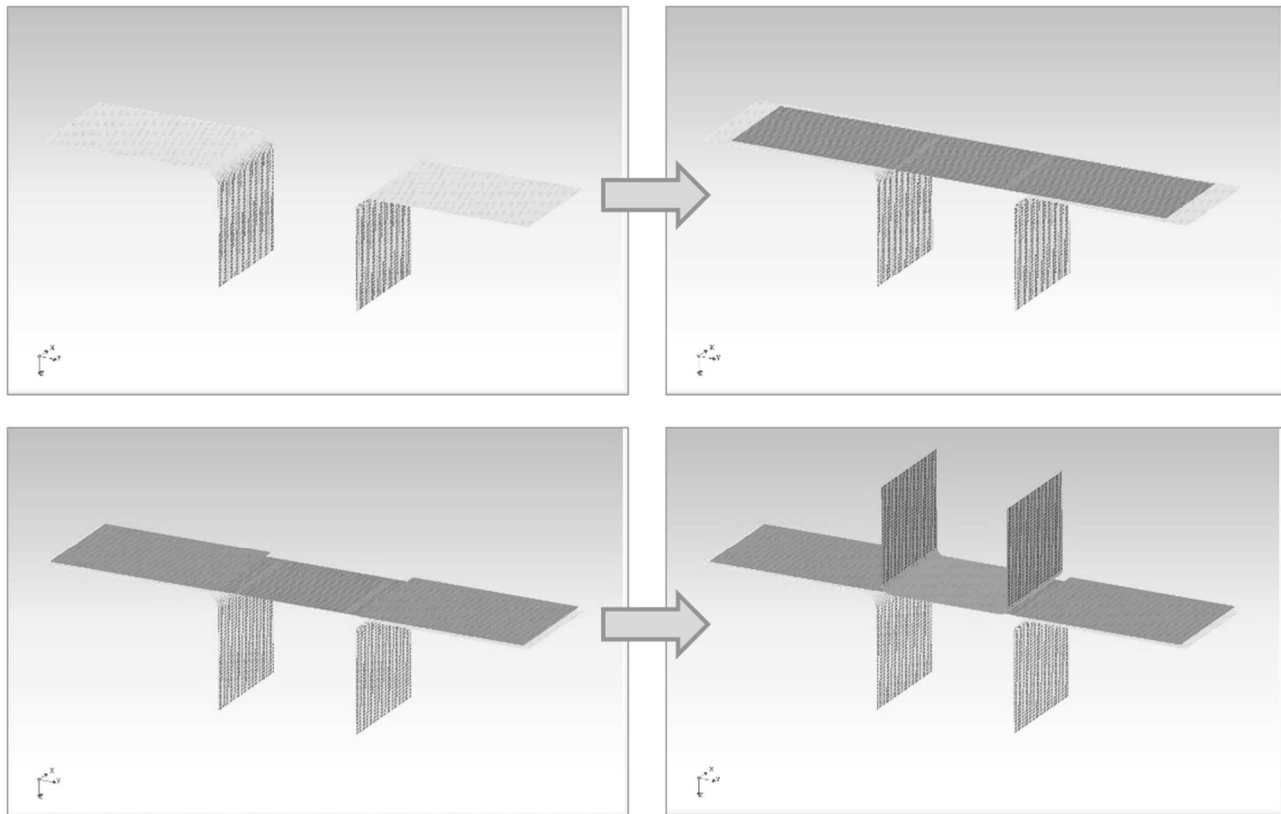


Fig. 12 Definition of the kinematic „Yoshida“ hardenign law – sw PAM-STAMP 2G

The next step after the definition of yield locus was the numerical simulation of given metal forming process. Using numerical simulation in sw PAM-STAMP 2G, the sheet metal forming process was implemented, specifically the bending technology – U-bending process. To set up the numerical simulation, it was first necessary to import all the needed parts of

forming tool and the given sheet blank, which was made using the blank editor in the sw PAM-STAMP 2G. The own U-bending process was performed using a simple bending punch, bending die and blank-holder. Subsequently, their relative positions were adjusted to correspond with the real metal sheet forming process – see Fig. 13.



**Fig. 13** Setting the position of individual tool parts – sw PAM-STAM 2G

Next, the forming process itself was set up. For each functional part involved in the forming process it was necessary to set and define boundary conditions in relation to the formed material, kinematic quantities

and process parameters. After setting all the necessary parameters, the computation of strain for the given sheet metal forming process with subsequent material spring-back was performed - see Fig. 14 and Fig. 15.

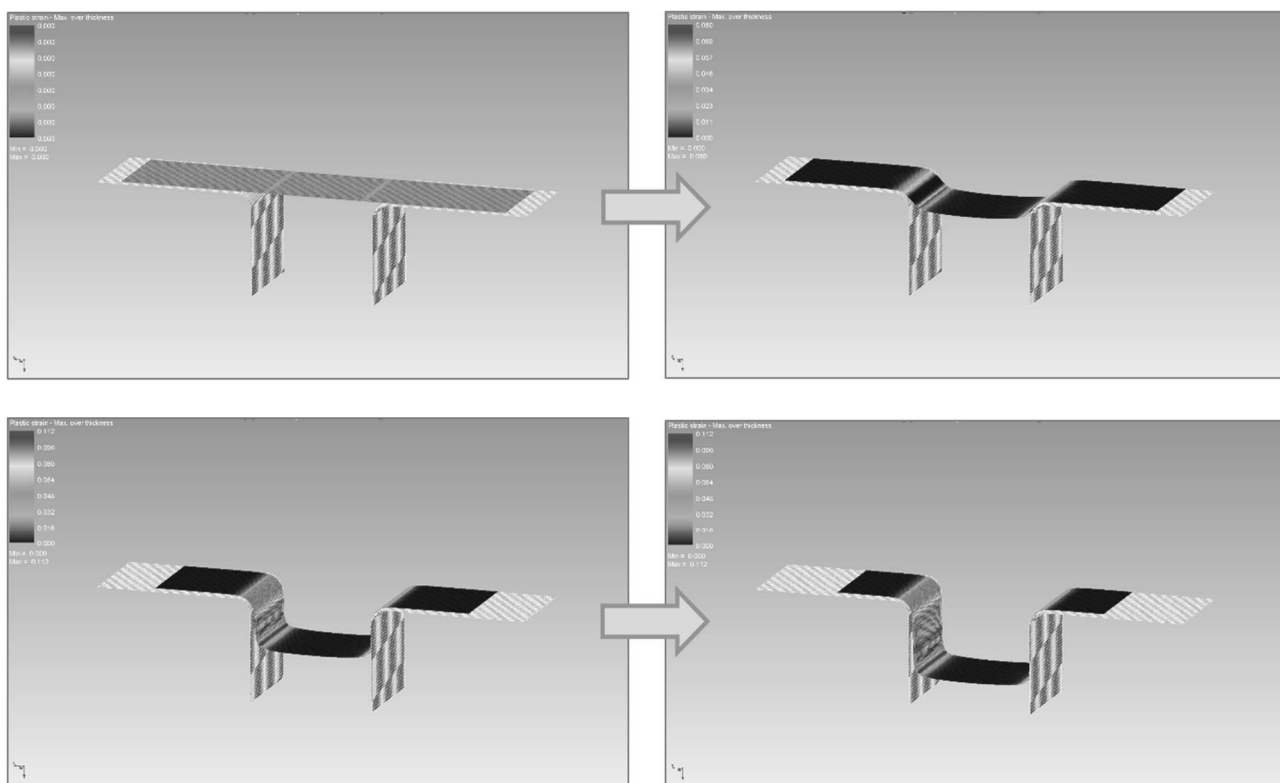


**Fig. 14** Course for the forming process numerical simulation – sw PAM-STAM 2G

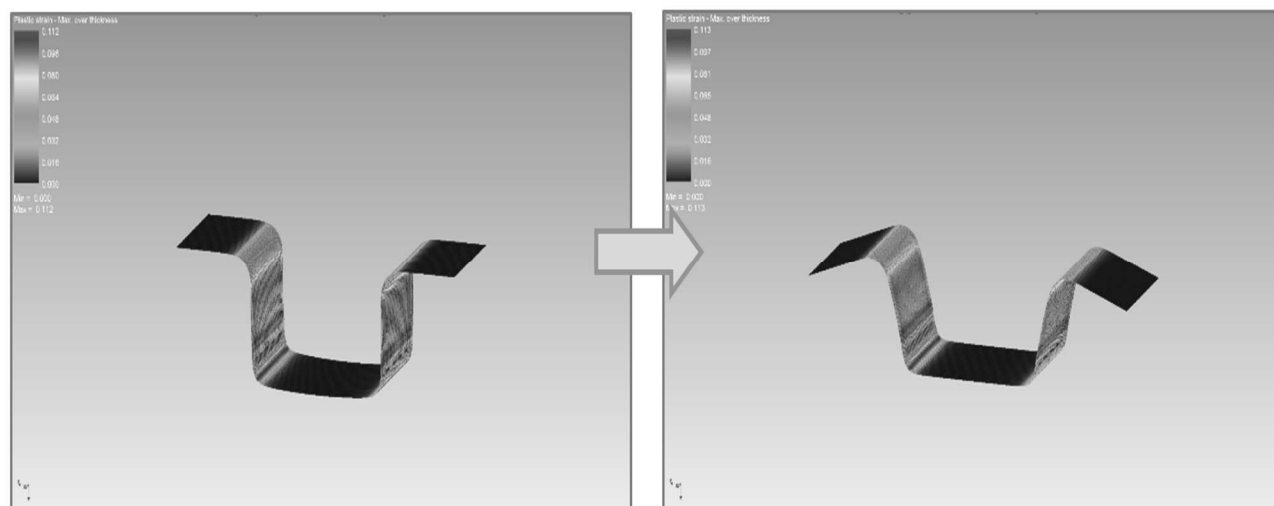
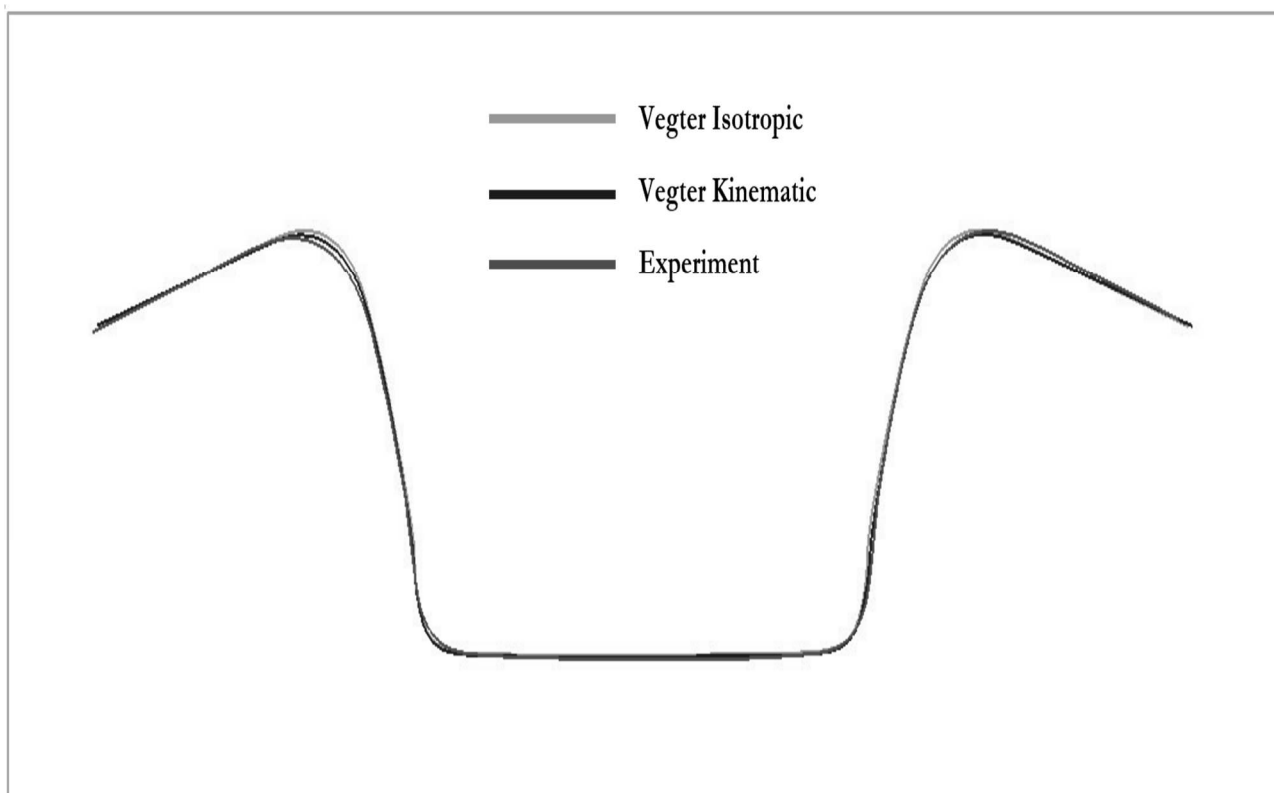


**Fig. 15** Spring-back of the stamping – sw PAM-STAMP 2G

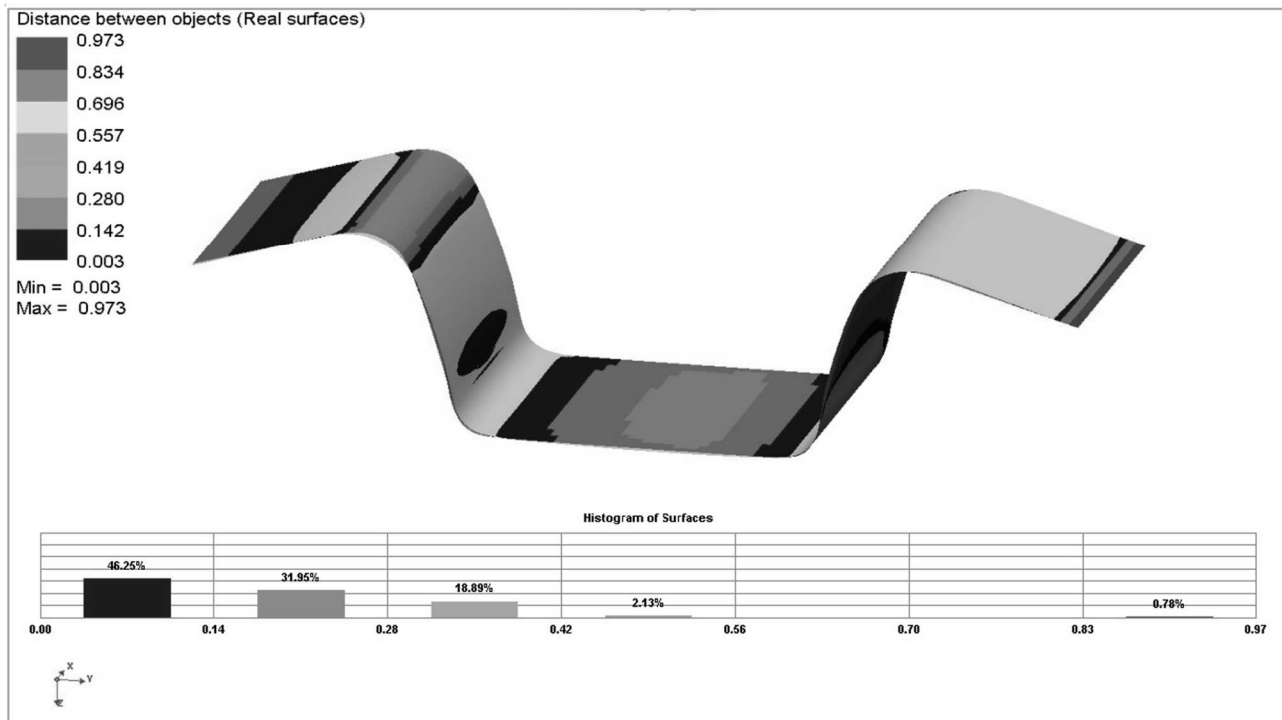
## 4 Results

Fig. 16 illustrates the comparison of the final sheet contour determined by computation of the numerical simulation in sw PAM-STAMP 2G according to the Vegter Standard Yield locus in the variant with isotropic and kinematic hardening law. Such numerical simulation computation is compared with the contour of real stamping prepared by the forming process. Based upon such comparison, small deviations between the numerical simulation according to the isotropic and kinematic hardening law can be observed. In the case of comparing these

results with respect to the real metal forming process, it can be seen that the kinematic hardening law better describes the shape and the spring-back angle with respect to the real stamping. The next Fig. 17 shows a visualization of the such deviations between the numerical simulation computation according to the Vegter Standard kinematic hardening law and the contour determined by the real sheet metal forming process. From the relevant histogram, it can be seen that most of the differences between the numerical simulation computation and the real forming process occur in the interval of 0 to 0.2 mm.



**Fig. 16** Final contours of the stamping from yield locus Vegter Standard with isotropic and kinematic hardening law regarding the contour of the real stamping



**Fig. 17** Deviations between the numerical simulation (Vegter Standard Kinematic Hardening law) and real stamping

## 5 Conclusion

This paper was focused on the use of sheet metal forming process mathematical modelling in the numerical simulation environment of sw PAM-STAMP 2G. Taking into account the current requirements and trends in the automotive industry, there was investigated a two-phased steel DP500. This material was used as it offers a favourable strength to weight ratio while maintaining sufficient formability for the metal forming process. In order to study the deformation behaviour of the material by numerical simulation, it was first necessary to provide correct material data, which enters the numerical simulations in the form of chosen yield locus (plasticity law). The required material characteristics were determined through selected material tests and then implemented into the material card in numerical simulation. After all the parameters of the numerical simulation were set, the actual computation of the U-bending process as well as the subsequent material spring-back took place. The computation was carried out with respect to the selected yield locus Vegter Standard in the variant with isotropic and kinematic hardening law during deformation of tested material.

Using numerical analysis of the forming process, the yield locus Vegter Standard with isotropic hardening law and Vegter Standard with kinematic hardening law (so-called "Yoshida" hardening law), were compared. The models based on the Vegter yield locus are generally considered to be among the newest material models currently used for computation the forming process and subsequent material spring-back

in sw PAM-STAMP 2G. Using the submitted research, both of these models can be classified as highly accurate, however it can be observed that combination of the Vegter Standard yield locus and kinematic hardening law provides more accurate results both for deformation and subsequent material spring-back. This is certainly due to the taking into account also influence of the Bauschinger effect in the forming process. Thus as a final statement, there can be concluded that if there are required highly accurate results for stampings undergoing more complex deformation, the use of the kinematic hardening law is very favourable in the area of developed plastic deformation.

## Acknowledgement

***This research was funded by the Institutional Endowment for the Long Term Conceptual Development of Research Institutes, as provided by the Ministry of Education, Youth and Sports of the Czech Republic.***

## References

- [1] DAVIES, Geoffrey. *Materials for Automobile Bodies*. B.m.: Elsevier, 2003. ISBN 978-0-08-047339-0.
- [2] Dual Phase (DP) Steels. *WorldAutoSteel* [online]. [vid. 2021-02-22]. Available from: <https://www.worldautosteel.org/steel-basics/steel-types/dual-phase-dp-steels/>

- [3] MARSHALL. Dual-Phase Steels: An Introduction. *National Material Company - Steel Processing Facilities* [online]. 23. březen 2018 [vid. 2021-02-22]. Available from: <http://www.nationalmaterial.com/introduction-dual-phase-steels/>
- [4] KUČEROVÁ, LUDMILA, IVETA CHENA, ADAM STEHLÍK. Effect of various heat and thermo-mechanical treatments on low alloyed CMnAlNb high strength steel. *Manufacturing Technology* [online]. 2021, 21. Available from: doi:10.21062/mft.2021.094
- [5] HAJSMAN, JAN, LUDMILA KUČEROVÁ, KAROLÍNA BURDOVÁ. Comparison of high strength steels with different aluminium and manganese contents using dilatometry. *Manufacturing Technology* [online]. 2020, 20, 436–441. Available from: doi:10.21062/mft.2020.060
- [6] SU, CHUNJIAN A XUETAO WANG. Sprinkback Research of V-type Sheet Metal forming based on the Adjustable Drawbead and Variable Blank-holder Force Cooperative Control Technology. *Manufacturing Technology* [online]. 2014, 14, 618–625. Available from: doi:10.21062/ujep/x.2014/a/1213-2489/MT/14/4/618
- [7] ESI GROUP. *PAM-STAMP 2G 2018 User's Guide*. B.m.: ESI Group. 2018
- [8] MACHÁLEK, JAKUB, RADEK, BARBORA FRODLOVÁ. *SIMULACE PROCESŮ PLOŠNÉHO TVÁŘENÍ V SOFTWARE PAM-STAMP 2G*. B.m.: Vysoká škola báňská - Technická univerzita Ostrava, 2012. ISBN 978-80-248-2715-5.